Electronic Supplementary Information

A Continuing Tale of Chirality：Metal Coordination Extended Axial Chirality of 4, 4'-Bipy to 1D Infinite Chain under Cooperation of Nucleotides Ligand

Pei Zhou, Jian-feng Yao, Chuan-Fang Sheng and Hui Li*

Key Laboratory of Cluster Science of Ministry of Education, School of Chemistry, Beijing Institute of Technology, No.5 South Street, Zhongguancun, Beijing 100081, P. R. China.

*E-mail address: lihui@bit.edu.cn

Tel: 86-10-68912667

Contents

1. IR spectra

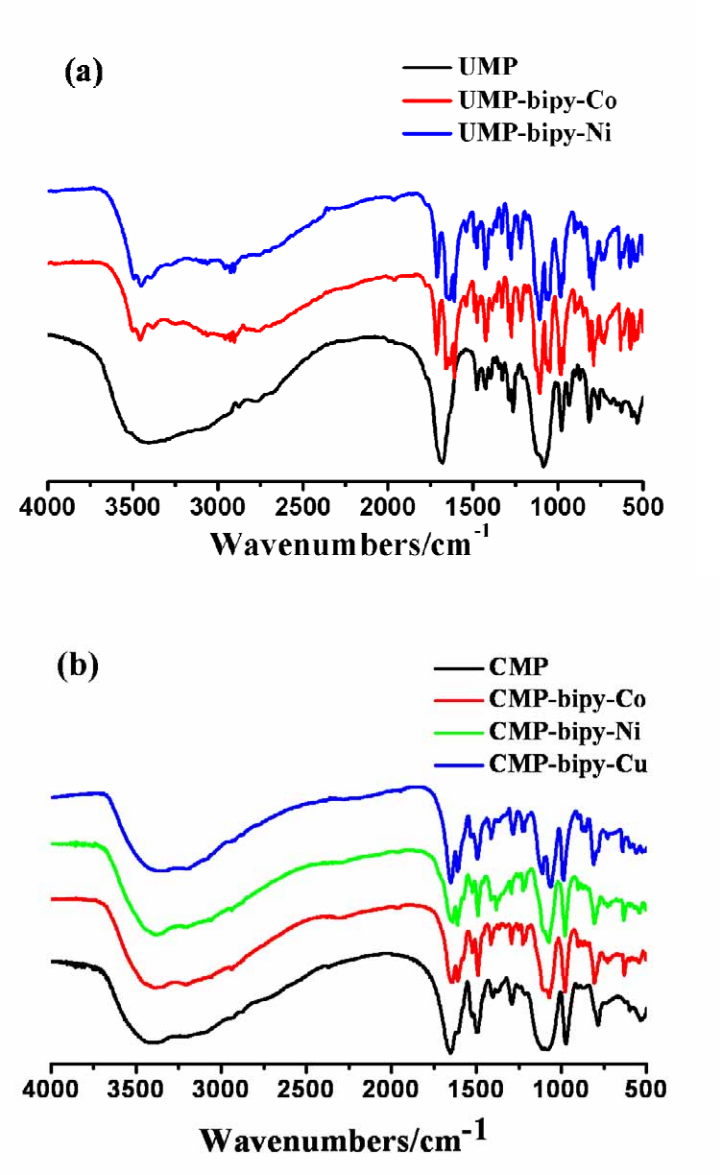

Figure 1S. IR spectra of (a) UMP Ligand and its complexes **1, 4;** (b)CMP ligands and its complexes **2, 3, 5.**

2. Structural Information for 1 – 5

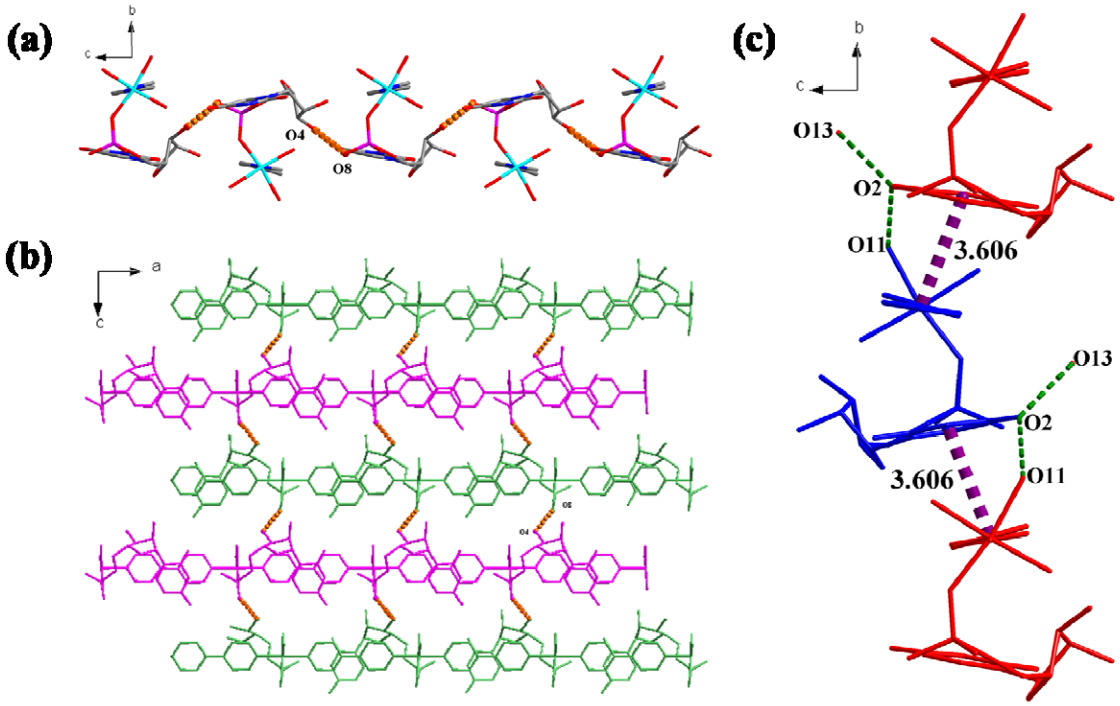

Figure 2S. (a) 2D chiral supramolecular architectures formed by hydrogen bonding (O4-H4A …O8, 2.674Å, 165.21°) view down from ***a*** axis. (b) The model of square grid 2D chiral supramolecular architectures of complex **1** on ac plane. (c) π-π stacking and intermolecular hydrogen bonding between sheets.

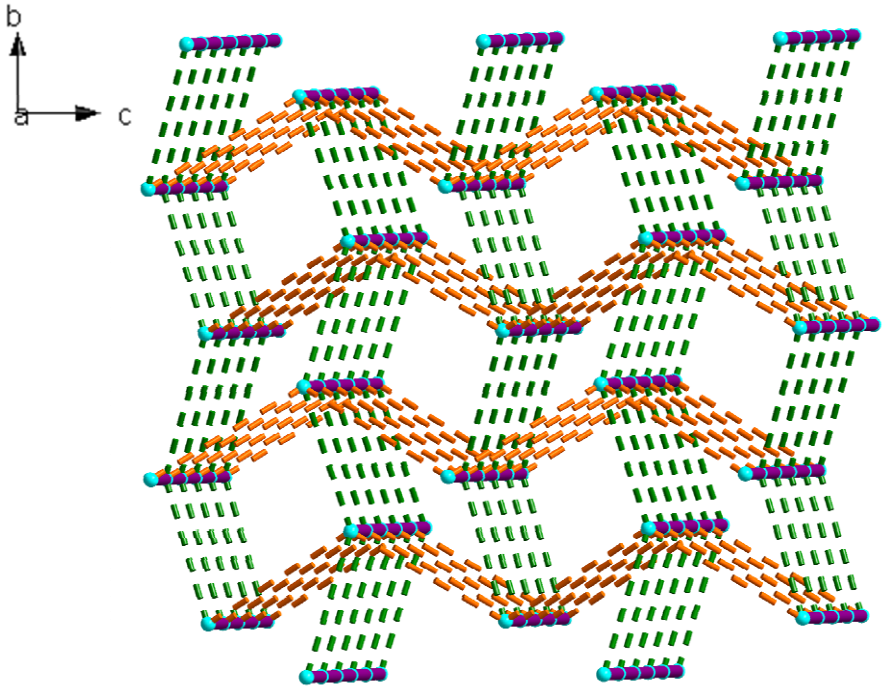

Figure 3S. Topology network of 3D supramolecular architecture of complex **1**. Dotted lines represent the Co-Co distances formed by interlinear noncovalent interaction. (yellow for interlinear hydrogen bonding O4-H4A …O8, and green for π-π stacking and inter-layer hydrogen bonding between sheets.).

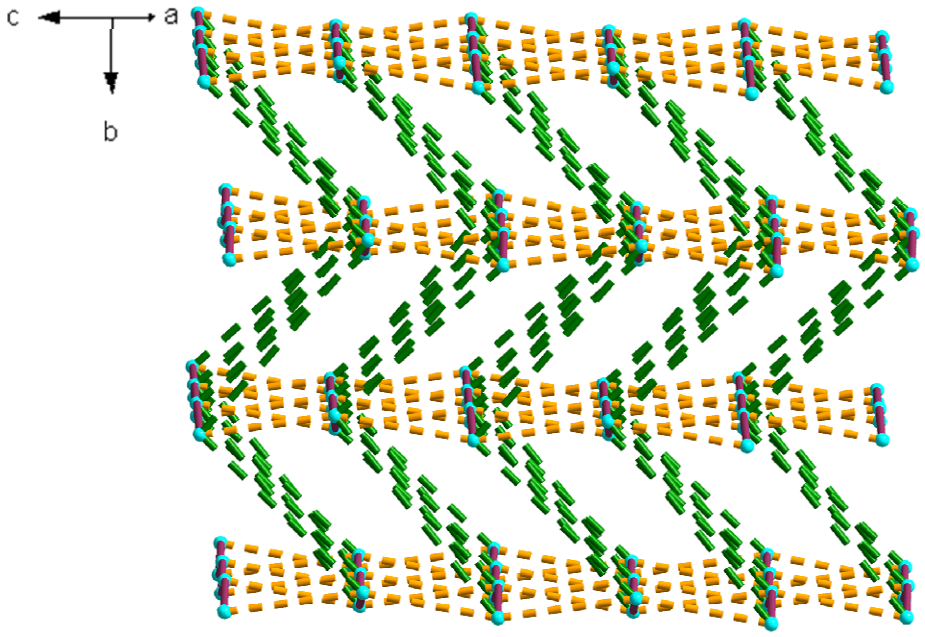

Figure 4S. Topology network of 3D supramolecular architecture of complex **2**. Dotted lines represent the Co-Co distances formed by interlinear noncovalent interaction (yellow for π-π stacking between chains, and green for inter-layer hydrogen bonding between sheets.).

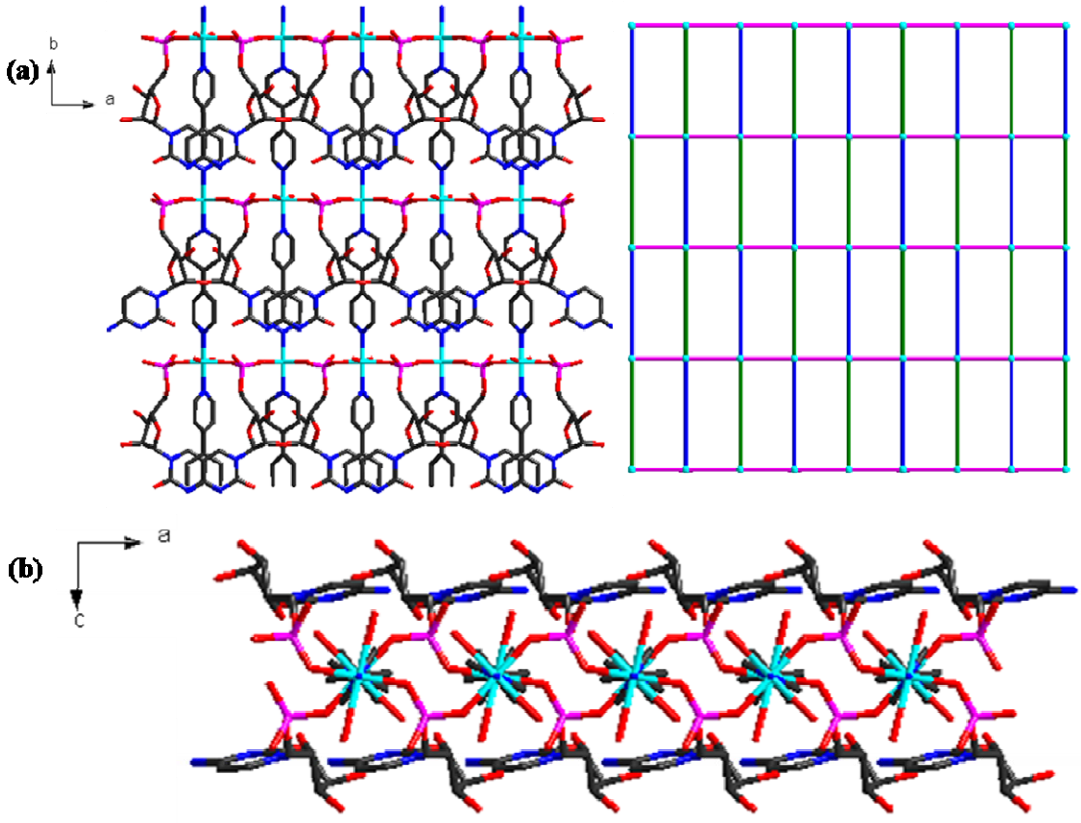

Figure 5S. (a) 2D coordination network and its topology architecture of complex **3**. (b) 2D layer of **3** view down from *b* direction. It is clearly that the CMP ligands arranged orderly above and below the plane in the same direction.

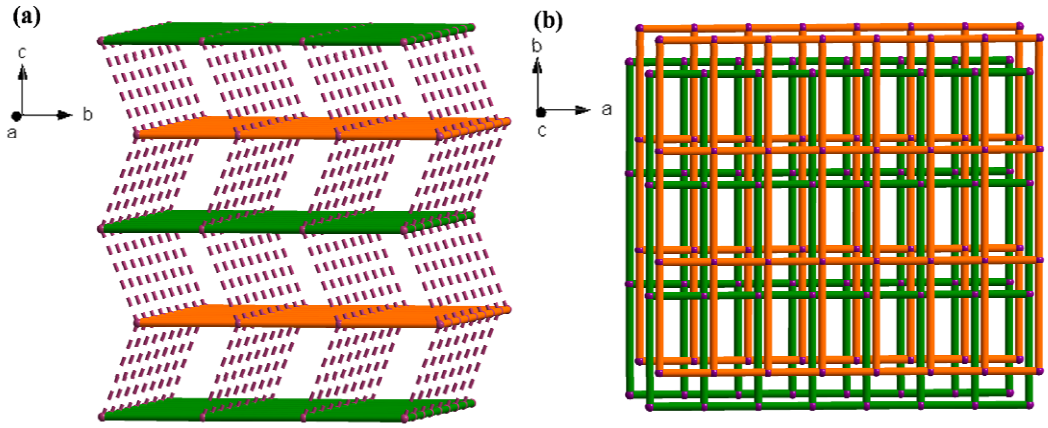

Figure 6S. Topology graph show the 3D supramolecular architecture of **3**. Purple lines represent the interlayer H-bonding.

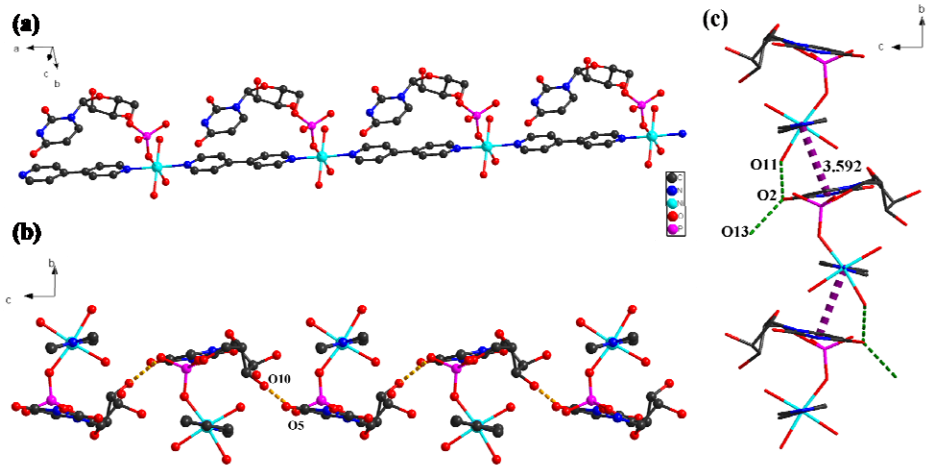

Figure 7S. (a) 1D coordination polymer of UMP-bipy-Ni **(4). (b)** 2D supramolecular sheet formed by inter-chain hydrogen bonding. (c) π-π stacking and inter-layer hydrogen bonding between sheets in complex **4**.

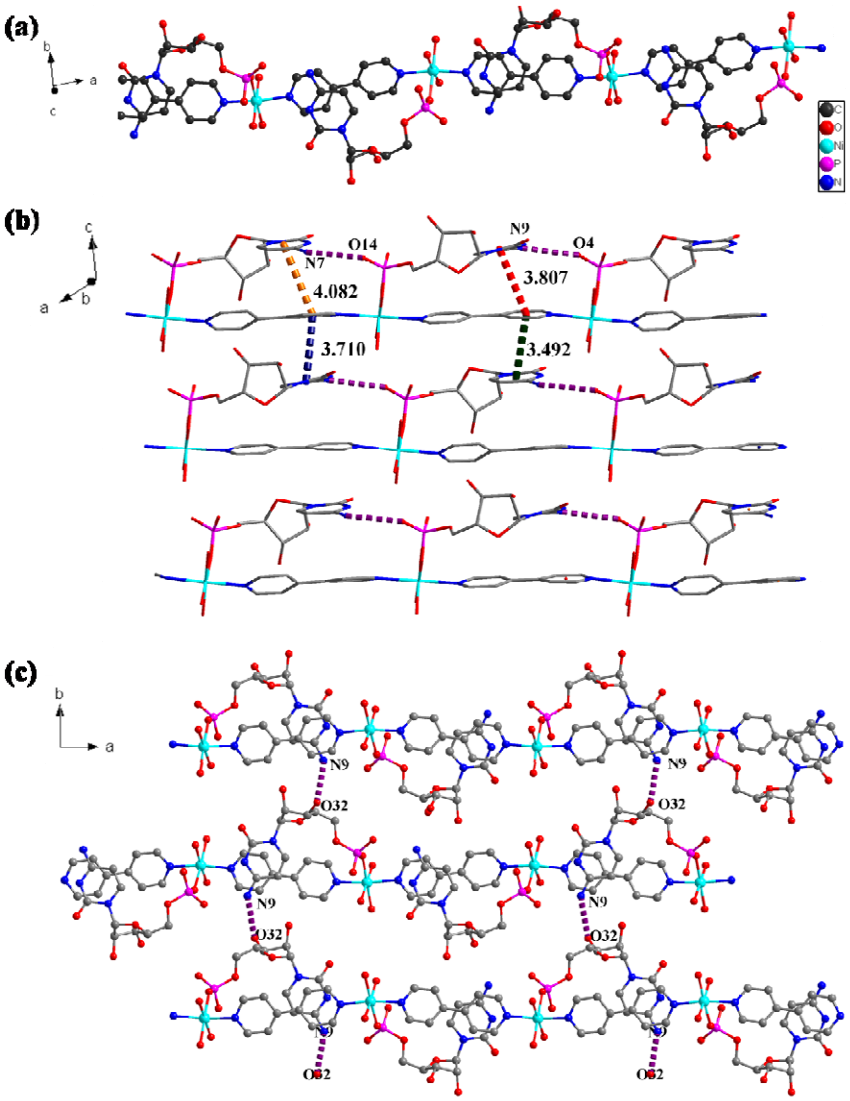

Figure 8S (a) 1D coordination polymer of CMP-bipy-Ni **(5). (b)** 2D layer formed by π-π stacking and intra-chain hydrogen bonding in complex **5**. (c) Inter-chain hydrogen bonds between sheets.

3. XRPD Patterns, CD and UV-vis spectra for 1-3

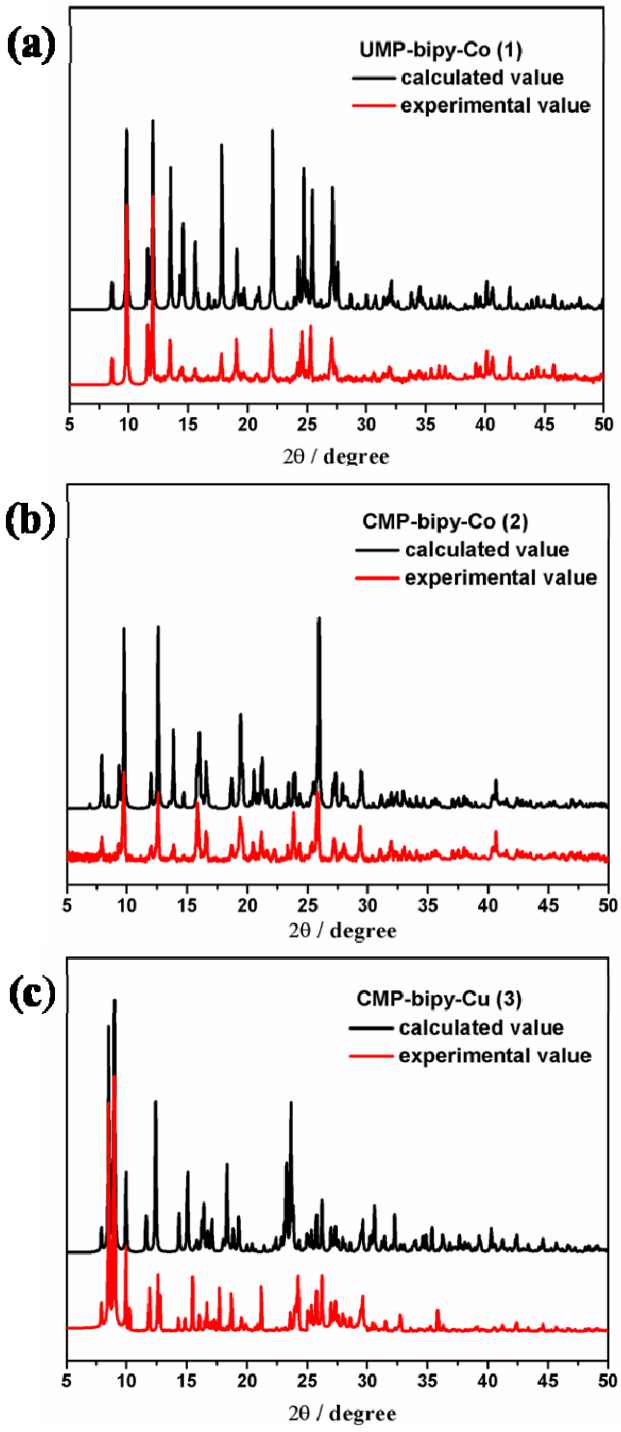

Figure 9S. PXRD patterns show the comparison between the experimental value and calculated ones for complexes **1-3**.

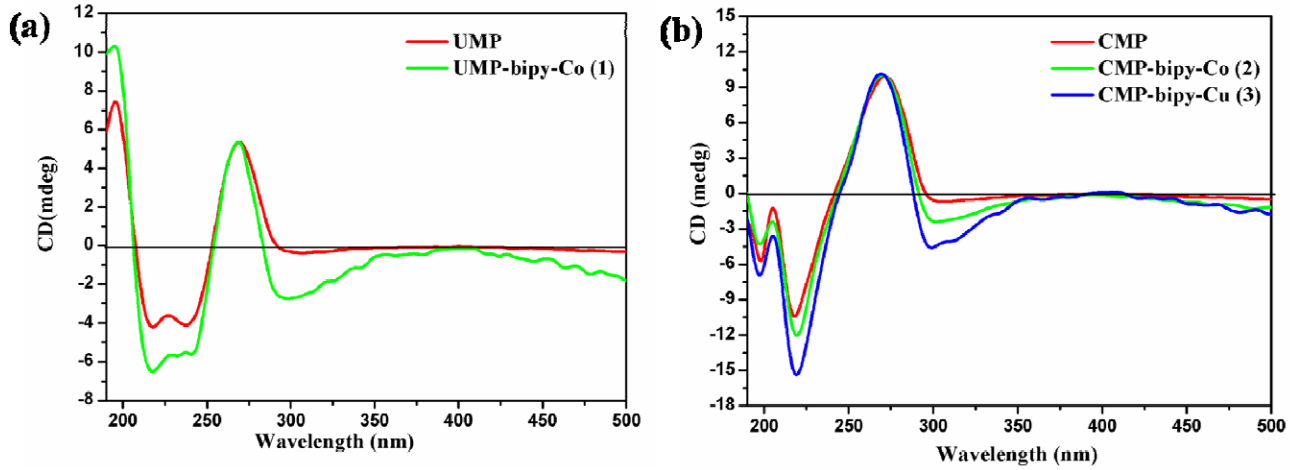

Figure 10S. The liquid-state CD spectra of nucleotide ligands and their complexes in water at 20℃. (a) UMP ligand and its complexes **1**; (b) CMP ligand and its complexes **2** and **3**. The spectrum was obtained by measuring a 0.2mM solution in a 1mm cell. The typical CD spectrum illustrates that the nucleotides ligand is D-ribonucleotide, which has a positive band near 269nm for UMP and 271nm for CMP. The weak negative band centered at 300nm, which is absent in the spectra of nucleotides ligands, demonstrates the formation of coordination complexes. Because the coordination of metal ions with UMP/CMP ligands can prevent the mutarotation, making ligands keep the β-anomers in their complexes.

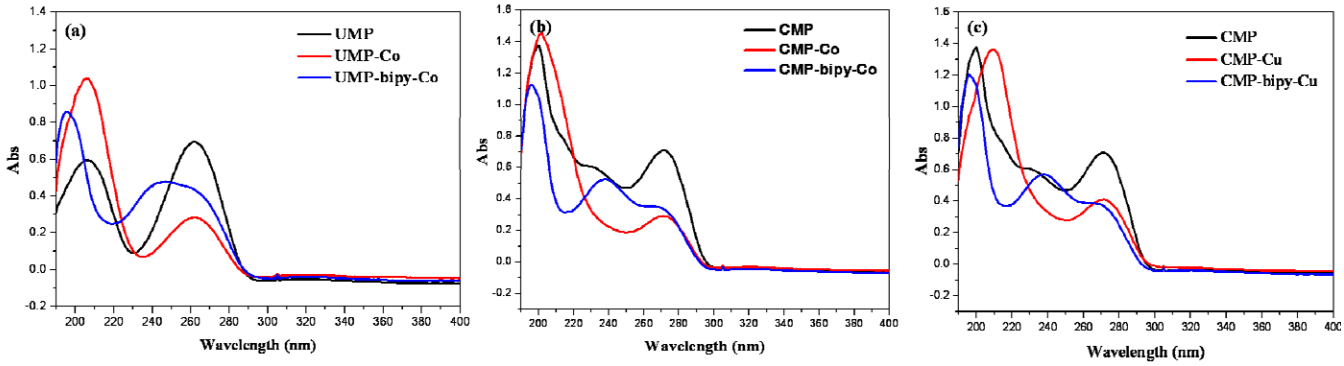

Figure 11S. UV-vis spectra of UMP, CMP, and their complexes. [L]=1.0×10^{-4} molL^{-1}, [L-M]=5.0×10^{-5} molL^{-1} (L:M=1:1, M=Co, Cu), [L-bipy-Co]=2.5×10^{-5} molL^{-1}, [L-bipy-Cu]= 5.0×10^{-5} molL^{-1} . Samples are dissolved in aqueous solution and the thickness of sample cell is 1cm. The band at 190~220nm in the UV-vis spectra of nucleotides ligands is due to the presence of the sugar moiety; 220~250 for n-π* transitions, and a broad band near 270nm for strong π-π* transition. Blue shift of the absorption for sugar moiety and a new peak at about 240nm in the spectra of UMP/CMP-bipy-M (M=Co and Cu) demonstrates the formation of ternary complexes.

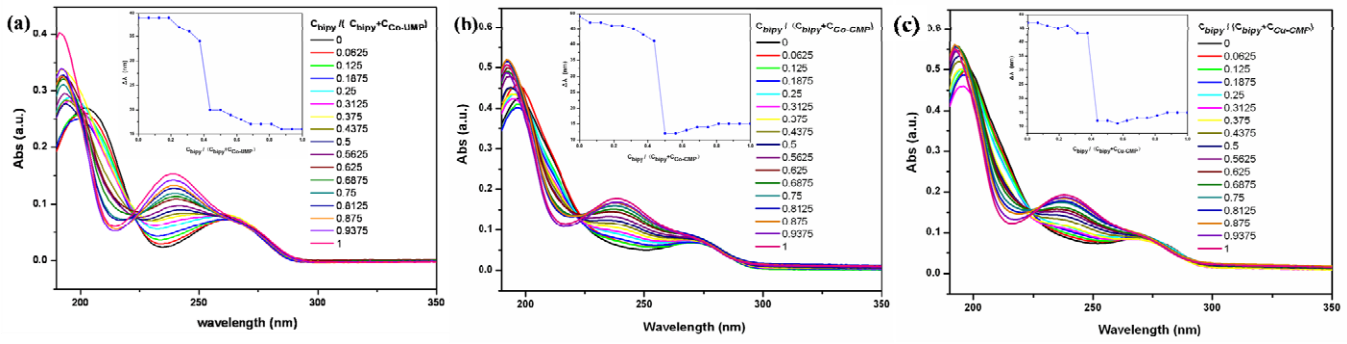

Figure 12S. Electronic spectra of M-NMP (1:1, M=Co^{2+} or Cu^{2+}, NMP=UMP or CMP) upon addition of 4, 4'-bipy. The total concentration of M-NMP and 4, 4'-bipy is held fixed ($C_{bipy}+C_{M\text{-}NMP}=1.0\times10^{-5}$M) varying the ratio of the components ($C_{bipy}/C_{M\text{-}NMP}$). The absorption intensity increased apparently as the concentration of 4, 4'-bipy increased and an isobathic point appeared at 223nm, which indicated the formation of the new system of M-NMP-4, 4;-bipy. (insert) Plot of the complex formation of M-NMP with 4, 4'-bipy, monitored with a UV spectrophotometer. The inflection point at about $C_{bipy}/ C_{bipy}+C_{M\text{-}NMP}=0.5$ indicating the formation of 1:1 adducts.

4. Magnetic property measurements for 3.

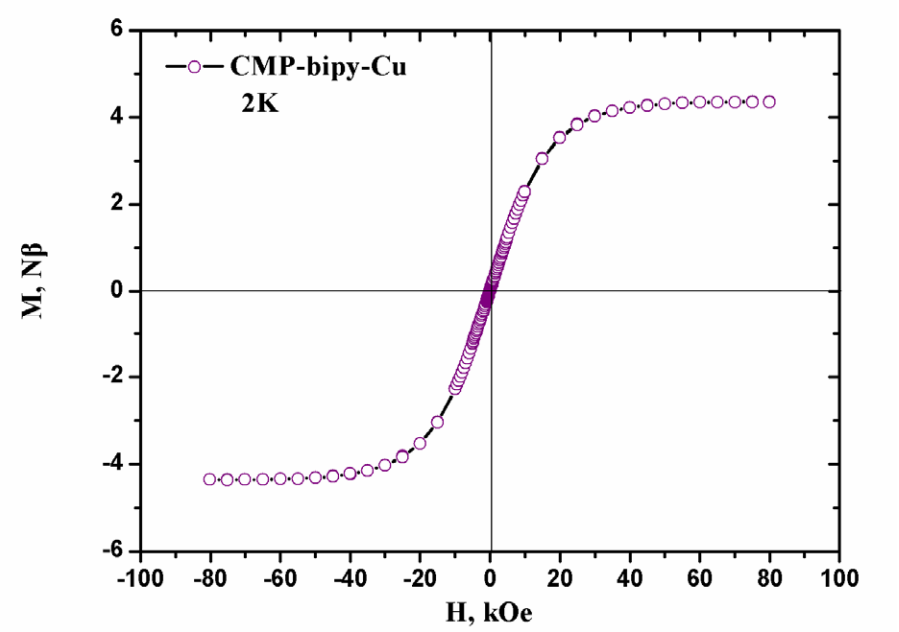

Figure 13S. Isothermal magnetization curves at 2K for **3**.

5. Tables for Crystal Data and H-bonding

Table 1S. Crystal Data and Structure Refinement of Complexes **1-5**

Complex	**1**	**2**	**3**	**4**	**5**
Empirical formula	$C_{19}H_{27}N_4O_{13}PCo$	$C_{38}H_{74}N_{10}O_{33}P_2Co_2$	$C_{38}H_{74}N_{10}O_{33}P_2Cu_2$	$C_{19}H_{27}N_4O_{13}PNi$	$C_{38}H_{74}N_{10}O_{33}P_2Ni_2$
Formula weight	609.35	1378.87	1280.00	609.13	1378.43
Wavelength (Å)	0.71073	0.71073	0.71073	0.71073	0.71073
Temperature(K)	153.15(2)	153.15(2)	153.15(2)	153.15(2)	153.15(2)
Crystal system	Orthorhombic	Monoclinic	Orthorhombic	Orthorhombic	Monoclinic
space group	$P2_12_12_1$	$P2_1$	$C222_1$	$P2_12_12_1$	$P2_1$
a (Å)	11.359(2)	12.395(3)	10.924(2)	11.272(2)	12.387(3)
b (Å)	14.395(3)	18.092(4)	22.372(5)	14.383(3)	18.193(4)
c (Å)	14.726(3)	14.144(3)	20.725(4)	14.720(3)	14.163(3)
α (°)	90	90	90	90	90
β (°)	90	115.46(3)	90	90	115.87(3)
γ (°)	90	90	90	90	90
Volume ($Å^3$)	2407.8(8)	2863.7(10)	5064.9(18)	2386.6(8)	2872.0(10)
Z	4	2	4	4	2
$D_{calc.}$ (g/cm^{-3})	1.681	1.599	1.679	1.695	1.594
Abs coeff (mm^{-1})	0.857	0.74	1.005	0.958	0.816
F (000)	1260	1440	2656	1264	1444
θ Range /°	2.67-29.12	1.95-29.14	2.07-29.08	1.98-29.12	2.91-29.04
Reflections collected / unique	21109 / 6429	25364 / 13844	21860 / 6729	20982 / 6263	24983 / 13112
Completeness to theta	29.12, 99.6 %	29.14, 99.1 %	29.08, 99.5 %	29.12 , 98.4 %	29.04, 98.1 %
GOF on F^2	0.998	1.006	1.0452	0.993	1.064
R1,wR2 [I >2σ(I)]	0.0382, 0.0780	0.0609, 0.1142	0.0462, 0.1139	0.0406, 0.0897	0.0673, 0.1197
R1,wR2 (all data)	0.0461, 0.0813	0.0890, 0.1280	0.0550, 0.1186	0.0516, 0.0941	0.0998, 0.1379
Flack parameter	0.014(11)	0.005(15)	0.025(16)	0.009(2)	0.022(17)

Table 2S. Hydrogen Bond Distances (Å) and Angles (deg) in **1-3.**

D-H···A	d(D-H)	d(H···A)	d(D···A)	∠(DHA)	Symmetry transformation for acceptor
			1		
Inter-chain hydrogen bonds					
O4-H4A ···O8	0.820	1.873	2.674	165.21	x, y, z
Inter-layer hydrogen bonds					
O13-H13E···O2	0.850	2.028	2.869	170.18	-x+1/2, -y+1, z+1/2
O11-H11A···O2	0.820	2.091	2.875	159.88	-x, y-1/2, -z+3/2
			2		
Intra-chain hydrogen bonds					
N7-H7A···O6	0.860	2.257	3.087	162.29	x, y, z
N10-H10B···O12	0.860	2.302	3.109	156.25	x+2, y, z+1
Inter-chain hydrogen bonds					
N10-H10C···O21	0.860	2.142	2.896	145.98	-x+2, y-1/2, -z+2
			3		
Intra-layer hydrogen bonds					
O8-H8···N11	0.850	2.136	2.795	134.03	x-1/2, y+1/2, z
N13-H13A···O3	0.860	2.236	2.951	140.52	x+1/2, y-1/2, z
Inter-layer hydrogen bonds					
O10-H10A···O26	0.820	1.938	2.711	156.86	x-1/2, -y+1/2, -z+2
O25-H25D···O2	0.850	1.930	2.780	178.64	x, -y+1, -z+2

Table 3S. Hydrogen Bond Distances(Å) and Angles(deg) in **4** and **5**

D-H···A	d(D-H)	d(H···A)	d(D···A)	∠(DHA)	Symmetry transformation for acceptor
			4		
inter-strand hydrogen bonds					
O10-H10A···O5	0.850	1.919	2.769	179.17	
Inter-layer hydrogen bonds					
O13-H13B···O2	0.850	2.052	2.852	156.38	-x+1/2, -y+1, z-1/2
O11-H11B···O2	0.820	2.104	2.893	161.19	-x+1, y-1/2, -z+3/2
			5		
Intra-chain hydrogen bonds					
N7-H7B···O14	0.860	2.252	3.084	162.75	x-2, y, z-1
N9-H9B···O4	0.860	2.259	3.063	155.57	x, y, z
Inter-chain hydrogen bonds					
N9-H9C···O32	0.860	2.150	2.906	146.45	-x+1, y-1/2, -z+2

Table 4S. Parameter about axial chirality of 4, 4'-bipy in complexes **4** and **5**

Complex	Dihedral angle of bipy (1)	Dihedral angle of bipy (2)	C-C bond length (Å)	π-π stacking (Å)
(1) UMP-bipy-Ni	6.7°		1.483	3.592
(2) CMP-bipy-Ni	4.3°	-19.7°	1.489, 1.500	4.082, 3.807 3.710, 3.492

Table 5S. Summary of Similarities and Differences for Complexes **1-3.**

	UMP-bipy-Co (1)	**CMP-bipy-Co (2)**	**CMP-bipy-Cu (3)**
Coordination sites	Phosphate group	Phosphate group	Phosphate group
Dimension	1	1	2
Chirality sources	Chirality of UMP; Axial chirality; Supramolecular helical chirality	Chirality of CMP; Axial chirality;	Chirality of CMP; Axial chirality;
Circle unit of 1D axial chirality	One bipy unit	Two bipy units	Two bipy units

Table 6S. Intra- and Intermolecular Hydrogen Bonds of Pyrimidine Rings in **1-3**.

D-H···A	d(D-H)	d(H···A)	d(D···A)	∠(DHA)	Symmetry transformation for acceptor
			1		
N2-H2···O7	0.860	1.951	2.802	170.05	x-1, y, z
O11-H11A···O2	0.820	2.091	2.875	159.88	-x, y-1/2, -z+3/2
O13-H13D···O1	0.850	1.978	2.820	170.19	x+1, y-1, z
			2		
O27-H27D···O2	0.833	2.102	2.807	142.26	x-1, y, z-1
O25-H25D···O2	0.850	2.135	2.985	179.19	x-1, y, z-1
O41-H41A···O2	0.841	2.103	2.944	177.86	x-1, y, z-1
N7-H7A···O6	0.860	2.256	3.086	162.30	x, y, z
N7-H7B···O28	0.860	2.192	2.938	145.02	-x+1, y+1/2, -z+1
N10-H10B···O12	0.860	2.304	3.110	156.20	x+2, y, z+1
N10-H10C···O21	0.860	2.145	2.897	145.92	-x+2, y-1/2, -z+2
O24-H24C···O1	0.850	1.973	2.821	174.53	x, y, z
O34-H34D···N6	0.850	1.924	2.773	177.50	x-1, y, z
			3		
N13-H13A···O3	0.860	2.236	2.951	140.52	x+1/2, y-1/2, z
N13-H13B···O23	0.860	2.397	3.186	152.79	x+1/2, y-1/2, z
O8-H8···N11	0.850	2.136	2.795	134.03	x-1/2, y+1/2, z